ELSEVIER

Composite Structures 61 (2003) 193–198

COMPOSITE STRUCTURES

www.elsevier.com/locate/compstruct

Size effects in the fiber pullout test

Qing-Sheng Yang [a], Qing-Hua Qin [b,c,*], Xi-Rong Peng [a]

[a] Numerical Simulation Center for Engineering, Department of Engineering Mechanics, Beijing University of Technology, Beijing 100022, China

[b] Department of Mechanics, Tianjin University, Tianjin 300072, China

[c] School of Aerospace, Mechanical and Mechatronic Engineering, The University of Sydney, Sydney, NSW 2006, Australia

Abstract

In this paper, a numerical simulation method is used to study the effect of specimen size on interfacial behavior of the specimen in fiber pullout tests. Interfacial shear stress and normal stress are analyzed for different sizes of the test specimen. The interface between fiber and matrix is assumed to be bonded perfectly. For simplicity, all materials are assumed to be linear and elastic solids, and the effects of thermal residual stress and friction between crack faces are ignored. The effects on interfacial behavior of both length of the fiber embedded in the matrix and thickness of the matrix around the fiber are studied using the finite element approach. Furthermore, the effect of the specimen size on the interfacial crack growth is also studied by way of energy release rate. The study shows that the size of the test specimen can influence interfacial stresses and fracture characteristics dramatically.

Keywords: Composite material; Interfacial stress; Energy release rate; FE simulation

1. Introduction

Interfacial properties play an important role in analyzing the mechanical behavior of fiber composites. The bonding characteristics of the interface between fiber and matrix have usually been investigated experimentally by examining some important physical parameters under various bonding situations. Two such experiments are the single fiber pullout test and the micro-drop debonding test [1–3]. The single fiber pullout test, introduced decades ago, is one representative method and has now become an important experimental technology in studying the mechanical behavior of fiber composites [1]. One of the obvious difficulties of this test is the determination of the distribution law of stresses over the interface, for example where strong stress gradients exist, as at the entry point (point A in Fig. 1) of the fiber composite and at the end of embedded part of the fiber (point B in Fig. 1). On the other hand, Some approximate approaches based on a shear-lag model can provide an approximate qualitative estimation for the stresses [3–5]. Unfortunately there is in the literature virtually no closed analytical solution of the interfacial stress, although its geometry is simple. This is because, in the elastic model, the maximum of interfacial stresses at points A and B may reach infinity, although in reality the interfacial stresses remain limited due to the large strain and plasticity effects. The actual maximum value is very complex and not easily obtainable by a simple analytical approach. The shear-lag scheme for interpretation of experimental data relies on very simplified theoretical ideas, mostly based on the assumption of constant shear stress distributions along the fiber length, and provides an approximation of interfacial shear and normal stresses. These values can only be average values of the interfacial stresses and cannot reveal the reality of the interfacial stress distributions along the fiber length. In addition, the initial crack at the interface may influence the interfacial behavior considerably. During the process of the fiber debonding from the matrix, crack growth process is very complicated due to the singularity of the stress field and the high stress concentration at the tips of the crack. The commonly used elastic shear strength of the interface cannot well describe the whole process of crack growth. However, it is convenient to apply the concept of the energy release rate to interpret the interfacial debonding. Following this line, many works have been done in applying fracture mechanics to micro-mechanics tests such as the fiber pullout test and

* Corresponding author. Address: School of Aerospace, Mechanical and Mechatronic Engineering, The University of Sydney, Sydney, NSW 2006, Australia. Tel.: +61-2-9351-7144; fax: +61-2-9351-7060.

E-mail address: qin@mech.eng.usyd.edu.au (Q.-H. Qin).

0263-8223/03/$ - see front matter
doi:10.1016/S0263-8223(03)00066-7

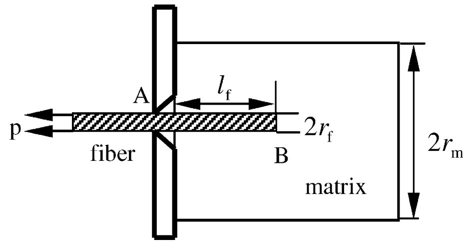

Fig. 1. Geometry model of the fiber pullout test.

the micro-drop debonding test, in order to simulate the whole process of the interface damage. These analyses can indeed explain the results of experiments very well [2–5]. Besides, thermal residual stress and friction of the crack in the interface may influence the debonding between fibers and matrices [6,7]. The presence of these effects constitutes a challenge in solving this category of problem, and the numerical simulation method used in this paper provides a powerful tool.

In what follows, a finite element (FE) simulation is performed to study the effect of specimen size (including embedded length, l_f, and radius, r_m, of wrapped matrix) on interfacial behavior of the specimen in fiber pullout tests. Both the fiber and the matrix are assumed to be linear elastic and the interface is assumed to be bonded perfectly. For simplicity, effects of thermal residual stress and friction between crack faces are ignored. It should be pointed out that the interfacial crack growth depends in some extent on the thermal residual stress and the friction between crack faces. For example, when the crack faces are under combined compression and shear, the effect of sliding frictional stresses on the crack faces can not always be ignored. Therefore the assumption above holds true when the near-tip contact zone is negligibly small and the residual thermal stress is relatively small in comparison with others. The numerical simulation includes analyses for interfacial shear and normal stresses with different dimensions of specimen. The process of interfacial crack growth is also studied by way of the energy release rate for different specimen sizes.

2. Finite element modeling

Consider a fiber–matrix specimen in the situation of fiber pullout test, whose geometry was shown in Fig. 1. The commercial FE software ANSYS is used in the FE simulation. Due to axisymmetry, the specimen can be considered as a 2-D elastic body and 8-node quadrilateral element PLANE82 is used in the analysis. Following parameters are used in all calculations [5]:

(1) Fiber: radius $r_f = 5$ μm, Young's modulus $E_f = 64$ GPa, Poisson ratio $\nu_f = 0.2$;
(2) Matrix: Young's modulus $E_m = 3$ GPa, Poisson ratio $\nu_m = 0.35$.

We distinguish following four cases:

(a) the effect of the embedded fiber length on interfacial behavior: $r_m = 10r_f$ and the embedded fiber length l_f varies from $2r_f$ to $40r_f$.
(b) the effect of wrapped thickness of the matrix (i.e. r_m) on interfacial behavior: $l_f = 10r_f$, while the wrapped thickness r_m varies from $2r_f$ to $30r_f$.
(c) the effect of the embedded fiber length on the process of the interfacial debonding: $r_m = 10r_f$, $l_f/r_f = 4$, 6, 8, 10, 15, 20, 30, and the crack length c varies from $0.05l_f$ to $0.95l_f$.
(d) the effect of the matrix wrapped thickness on the process of the interfacial debonding: $l_f = 12r_f$, $r_m/r_f = 4$, 6, 8, 10, 15, 20, 40, and the crack length c varies from $0.05l_f$ to $0.95l_f$.

The FE results and discussion are provided in the next two sections.

3. Interfacial stresses of fiber composites

The interfacial stresses of fiber composites under pullout test is usually determined by a shear-lag model in which stresses along the fiber length are assumed to be uniformly distributed. Actually, the variations of interfacial stress along the fiber are very complicated. For example, a high stress concentration exists near the critical points A and B of the fiber. Therefore, the FE mesh density has been increased near the two critical points (element size being less than 1/10 of the fiber radius in our analysis) in order to obtain a meaningful solution. A typical element mesh is shown in Fig. 2. With the commercial FE software ANSYS and the element mesh shown in Fig. 2, the first two cases in Section 2 are analyzed as follows.

Case (a): Fig. 3 shows the distribution of the shear stress along the fiber for different lengths l_f. It can be seen from the figure that shear stress reaches its maximum at point A (see Figs. 2 and 3). Along the fiber, the shear stress decreases rapidly to zero near the end point

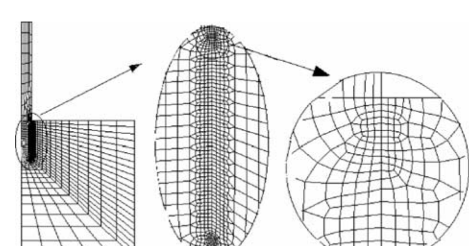

Fig. 2. FE mesh.

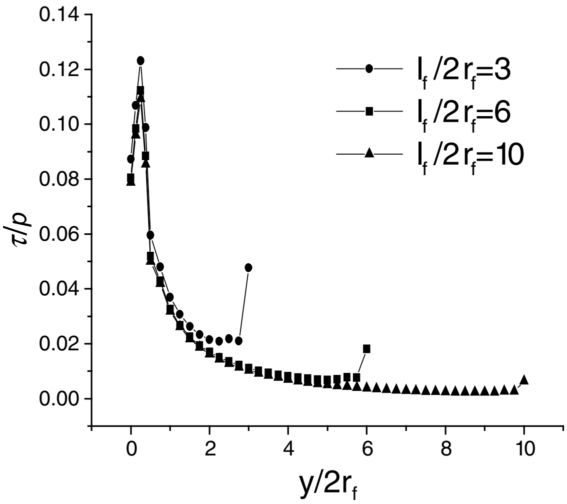

Fig. 3. Shear stresses along fiber for different fiber-embedded length.

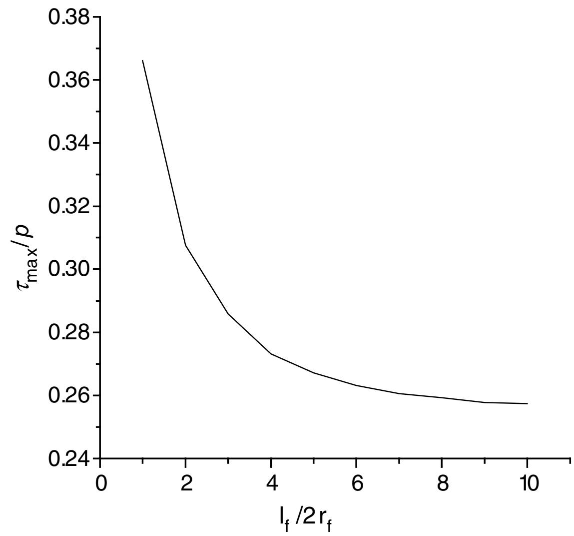

Fig. 5. Maximum shear stress vs fiber-embedded length.

of the fiber. Then, the shear stress increases suddenly near point B. It is shown that there is a stress concentration near both critical points A and B of the fiber. In Fig. 4 the normalized stress σ/p is presented as a function of normalized axial coordinate $y/2r_f$. It can be seen from the figure that the maximum of normal stress occurs also at point A of the fiber, which may be the cause of interfacial debonding. The stress drops to zero suddenly and then remains at zero up to the end of the fiber, at which another stress concentration occurs. The results in Fig. 5 show variation of maximum shear stress τ_{max}/p with the normalized embedded fiber length $l_f/2r_f$. It is evident from Fig. 5 that τ_{max}/p decreases gradually along with the increase in embedded fiber length. Moreover, the degree of stress concentration at point B also decreases (see also Figs. 3 and 4), but this tendency becomes weaker at a certain point even though the embedded length of fiber continues to increase. When the embedded length of fiber amounts to more than 20 times the fiber radius ($20r_f$), the stress concentration does not decrease any further (see Fig. 5). The stress concentration near point B is relatively high when the embedded length is small and relatively low when the embedded length is large.

Case (b): Figs. 6 and 7 show, respectively, the numerical results for the normalized shear and normal stresses versus the normalized axial coordinate $y/2r_f$. It is found that the stress concentration at point B is not very sensitive to the wrapped thickness r_m, as shown in these two figures. The calculation also indicates that the stress concentration near point B is attributable to the

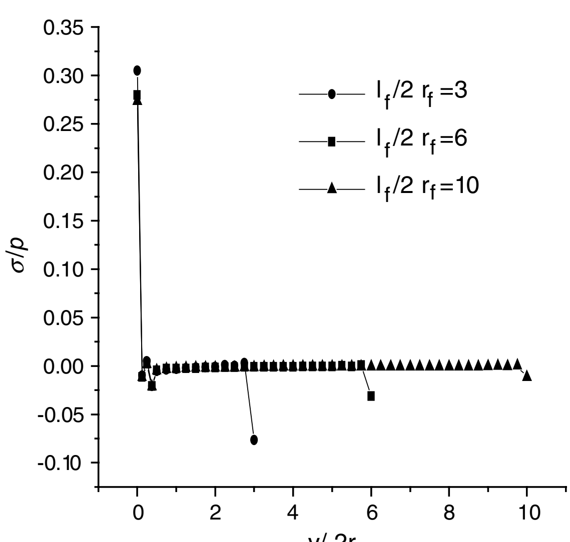

Fig. 4. Normal stresses along fiber for different fiber-embedded length.

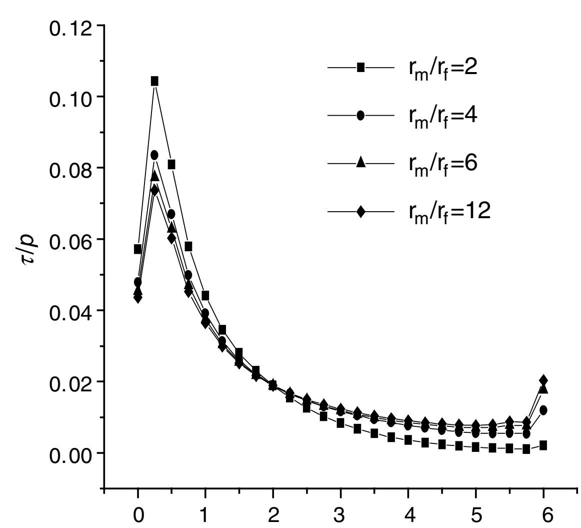

Fig. 6. Shear stresses along fiber for different matrix-wrapped thickness.

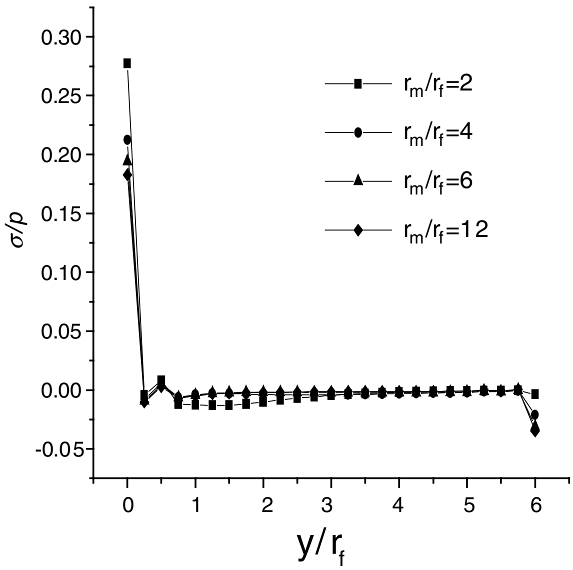

Fig. 7. Normal stresses alone fiber for different matrix-wrapped thickness.

embedded length only, not to the wrapped thickness. It is found from Figs. 6 and 7 that all curves intersect at a certain point ($y/r_f \approx 2$ in Fig. 6). This indicates that there is an optimal embedded length at which variation of the matrix-wrapped thickness does not affect interfacial stresses.

Fig. 8 shows that, for a fixed fiber-embedded length, the maximum of both interfacial shear stress and normal stress at point A are relatively larger when wrapped thickness is relatively small. The maximum of interfacial stresses decreases along with increase in the wrapped thickness. This tendency stops at a certain point even though the embedded length of fiber continues to increase, as shown Fig. 8.

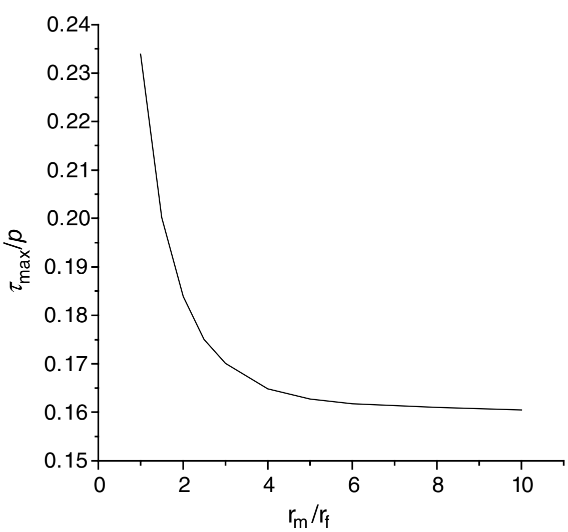

Fig. 8. Maximum shear stress vs matrix-wrapped thickness.

The numerical results above indicate that the concentration of shear stress on the interface is not the only factor implicated in interfacial damage. The concentration of normal stress vertical to the interface is another important factor.

4. Energy release rate of interfacial crack

The FE simulation for the relationship between energy release rate and crack length as well as the effect of specimen size on energy release rate is studied in this section. Because of singularity of the stress field at the tip of a crack, singularity elements [8] are used around the tip of a crack. FE mesh around the tip has also been refined so that minimum element size at the tip of the crack is 1% the fiber radius only. The local FE mesh and the singularity element at a crack tip are shown in Fig. 9. For a small crack length, deformation of free part of the fiber contributes significantly to the energy release rate. The energy release rate of this part can be expressed approximately by [6]

$$G_0 = \frac{p^2}{4\pi^2 r_f^3 E_f} \tag{1}$$

The numerical results for cases (c) and (d) described in Section 2 are listed in Figs. 10 and 11. The numerical study shows that when crack length is very small, the energy release rate decreases as the cracks increases. However, subsequently the energy release rate will increase instead of decreasing along with increase in crack length. It is also observed from Fig. 10 that a 'plateau range' appears during crack growth. When the crack approaches point B (see Fig. 1), the energy release rate increase quickly with a very high incremental rate. For the case of a relatively small embedded length, the plateau range cannot be seen; the length of the plateau range increases as the length of fiber embedded increases.

Fig. 11 shows the effect of the matrix-wrapped thickness on the energy release rate. When wrapped thickness is more than 20 times the fiber radius, the

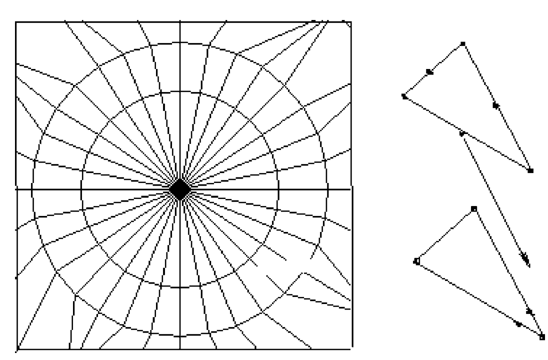

Fig. 9. Singularity elements arranged at the tip of crack.

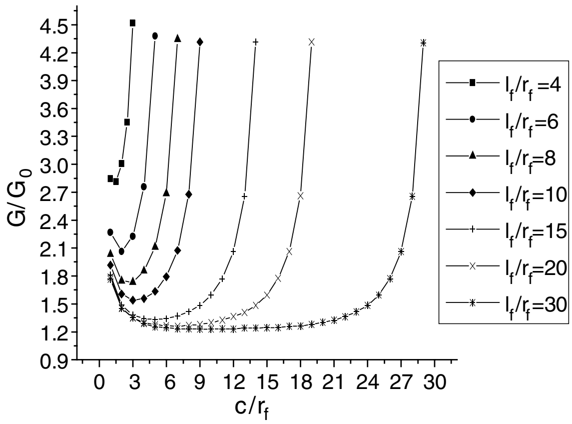

Fig. 10. Energy release rate for different fiber-embedded length ($r_m = 10r_f$).

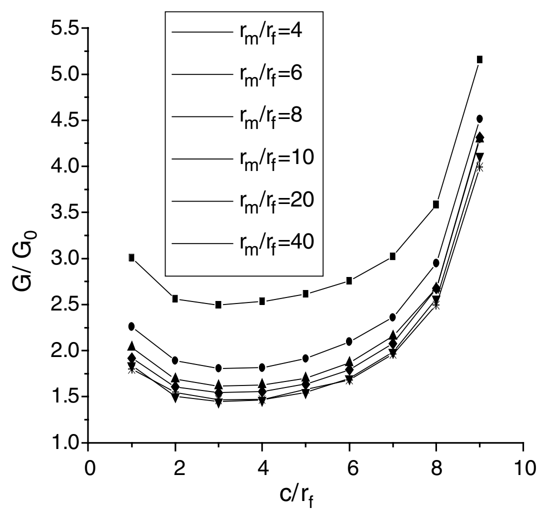

Fig. 11. Energy release rate for different matrix-wrapped thickness ($l_f = 12r_f$).

effect of wrapped thickness on energy release rate can be ignored. Approaching point A, energy release rate decreases gradually until it reaches its minimum. This indicates that within the domain of stress concentration, any small interfacial pre-crack will develop steadily to a certain length. After passing the critical crack length c_{cri}/r_f ($c_{cri}/r_f \approx 8$ in Fig. 11), the crack will grow unstably and this instability continues until the fiber is completely debonded from the matrix.

5. Conclusions

The effect of specimen size in the fiber pullout test was studied by FE simulation. The distributions of interfacial shear and normal stresses along the axial direction of the specimens were obtained by way of the commercial FE software ANSYS. The influence of specimen size on the energy release rate of interfacial cracks was also discussed in this study. Specimen size here includes the fiber-embedded length and the matrix-wrapped thickness. The results obtained can be used to establish relationships between fracture toughness and fiber-embedded length and/or matrix-wrapped thickness. For the case of catastrophic failure, the proposed numerical modeling can also be used to determine the critical load, P_c, as a function of embedded length. The findings of this work can be summarized as follows:

(1) Both normal and shear stresses are not constant along the interfacial length which was used. Normal and shear stress concentrations exist near the fiber ends. In contrast, in the shear-lag model the shear stress along the fiber was assumed to be constant.
(2) Interfacial shear and normal stresses are affected by the specimen size, i.e. embedded fiber-length and wrapped thickness. The stresses near point A become smaller along with decrease in fiber-embedded length or matrix-wrapped thickness. After a certain point, the interfacial stresses do not decrease. Figs. 6 and 7 show that all curves intersect at a certain point. This indicates that there is an optimal embedded length at which variation of the matrix-wrapped thickness does not affect interfacial stress.
(3) For a fixed interfacial crack length, the energy release rate (near point A) becomes small when the fiber-embedded length or the matrix-wrapped thickness increases. During the whole process of interfacial crack growth, the energy release rate experiences a 'plateau range' within a wide range of crack length. For example, the plateau width is from $c/r_f = 3$ to $c/r_f = 21$ for the curve $l_f/r_f = 30$ in Fig. 10. This indicates that energy release rate is approximately constant except for the domain near the two critical points (A and B). From the above analysis it is realized that fracture toughness should be obtained from specimens of full section embedded length and wrapped thickness to ensure relevant levels of constraint and thus realistic values of toughness. Therefore, full size specimens are recommended if accurate rather than conservative data are required.

References

[1] Favre JP. Characterization of fiber/resin bonding in composites using a pull-out test. Int J Adhes 1981;1:234–41.
[2] Beckert W, Lauke B. Critical discussion of the single-fiber pull-out test: Does it measure adhesion?. Compos Sci Technol 1997; 57:1689–706.
[3] Singletary J, Lauke B, Beckert W. Examination of fundamental assumptions of analytical modeling of fiber pull-out test. Mech Compos Mater Struct 1997;4:95–112.
[4] Kessler H, Schuller T, Beckert W, Lauke B. A fracture-mechanics model of the microbond test with interface friction. Compos Sci Technol 1999;59:2231–42.

[5] Schuller T, Beckert W, Lauke B. A finite element model to include interfacial roughness into simulations of micromechanical tests. Compos Mater Sci 1999;15:357–66.
[6] Outwater JO, Murphy MC. Fracture energy of unidirectional laminates. Modern Plast 1970;47:160–9.
[7] Beckert W, Lauke B. Fracture mechanics finite element analysis of debonding crack extension for single fiber pull-out specimen. J Mater Sci Lett 1995;14:333–6.
[8] Anderson JL. Fracture mechanics: fundamentals and applications. Boston: CRC Press; 1991.